(Preprint) AAS

STRUCTURE DETECTION METHOD FOR SOLVING STATE VARIABLE INEQUALITY PATH CONSTRAINED OPTIMAL CONTROL PROBLEMS

Cale A. Byczkowski* **and Anil V. Rao†**

A structure detection method is developed for solving state-variable inequality path constrained optimal control problems. The method obtains estimates of activation and deactivation times of active state-variable inequality path constraints (SVICs), and subsequently allows for the times to be included as decision variables in the optimization process. Once the identification step is completed, the method partitions the problem into a multiple-domain formulation consisting of constrained and unconstrained domains. Within each domain, Legendre-Gauss-Radau (LGR) orthogonal direct collocation is used to transcribe the infinite-dimensional optimal control problem into a finite-dimensional nonlinear programming (NLP) problem. Within constrained domains, the corresponding time derivative of the active SVICs that are explicit in the control are enforced as equality path constraints, and at the beginning of the constrained domains, the necessary tangency conditions are enforced. The accuracy of the proposed method is demonstrated on a well-known optimal control problem where the analytical solution contains a state constrained arc.

INTRODUCTION

In the past two decades, direct collocation methods have become increasingly popular for obtaining numerical solutions to optimal control problems.[1] In a direct collocation method, the state and control are approximated by a set of basis functions, and the constraints are enforced at selected collocation points on the time interval of interest. The original infinite-dimensional optimal control problem is then transcribed into a large sparse nonlinear programming problem (NLP), and the NLP is solved using well-known software.[2,3] A particular class of collocation methods that have been developed in the past decade is the class of Gaussian quadrature orthogonal collocation. The most well developed Gaussian quadrature collocation methods use either Legendre-Gauss (LG) points,[4] Legendre-Gauss-Radau (LGR) points,[5,6] or Legendre-Gauss-Lobatto (LGL) points.[7] It has been shown that when the solution of an optimal control problem is smooth, Gauss quadrature methods converge at an exponential rate.[8] Conversely, when the solution of an optimal control problem is either nonsmooth or singular, more involved adaptations of Gaussian quadrature collocation must be considered in order to obtain an accurate solution in a computationally efficient manner. In the past decade, a class of so called hp-adaptive mesh refinement methods have been developed to improve the solution accuracy to problems whose solutions are nonsmooth.[9–13] Although these techniques greatly improve accuracy and computational efficiency when solving an optimal control problem whose solution is nonsmooth, it still may be the case that these techniques place an unnecessarily large number of collocation points near any discontinuity in the solution. One particular class of optimal control problems whose solution may be nonsmooth and for which these previous techniques may produce an unnecessarily large mesh is a state-variable inequality constrained (SVIC) optimal control problem. This paper focuses on developing a strategy for accurately solving SVIC optimal control problems.

Pure state-variable inequality constraints have routinely caused difficulty in solving optimal control problems. Since the early 1960s, various necessary conditions have been derived to provide guidelines for handling such constraints.[14–17] Since then, a variety of methods have been developed to solve SVIC problems,

*Ph.D. Student, Department of Mechanical and Aerospace Engineering, University of Florida, Gainesville, FL 32611.
†Professor, Department of Mechanical and Aerospace Engineering, University of Florida, Gainesville, FL 32611. Corresponding Author.

all falling within the framework of either an indirect or direct approach. Two of the most common indirect methods for solving SVIC optimal control problems are penalty function techniques[18–20] and transcription techniques.[21–23] In a penalty function method, the original inequality constrained optimal control problem is approximated by augmenting any inequality constraints to the cost functional through the use of a penalty term. This approximation, which is now unconstrained, is iteratively solved until the solution approaches the solution of the original problem. In a transcription method, the dimension of the state is increased through the inclusion of parametric variables (often referred to as "slack variables"). If the order of the inequality constraint is q, then the dimension of the state is also increased by q, and the additional state variables are defined such that the inequality constraint is satisfied at every point along the trajectory. Both methods benefit from the fact that no a priori knowledge of when the constraint becomes active is necessary, but suffer computationally as each need to employ some form of iterative process to obtain an accurate approximation of the solution. Note, the aforementioned methods are referred to as "indirect" since they typically involve an iterative procedure to approximate the solution. In a direct approach, the SVIC (or an appropriate time derivative) are directly adjoined to the problem.[24–27] Specifically, the SVIC and its $q-1$ time derivatives are enforced as equality constraints at the entry of a constrained arc, while the *q-th* time derivative is enforced as a mixed state/control equality constraint. A pitfall in using a direct approach is that the number and location of constraint activation/deactivation (A/D) points must be guessed.

This paper uses a direct approach for solving SVIC optimal control problems. The method alleviates the need to guess the number and location of A/D points. Specifically, a detection method is developed to obtain estimates of A/D times in the SVIC optimal control problem. The locations of A/D of the state inequality constraints are then used to partition the original time domain into multiple domains, and the estimated locations of the A/D points are included as additional decision variables in the NLP to be optimized when solving the partitioned problem. The method developed in this paper constructs the NLP through the use of a multiple-domain LGR collocation method,[28] which significantly improves the accuracy of the computed approximation to the SVIC optimal control problem as compared with advanced direct collocation methods.

The remainder of the paper is organized as follows. First, the general form of an optimal control problem in Bolza form is presented along with the necessary conditions for optimality when SVICs are present. Next, an overview of the multiple-domain LGR collocation method used in this research is shown, then the structure detection method developed in this research that is used for directly solving SVIC optimal control problems is described. Finally, the accuracy of the method developed in this research is demonstrated on a well known SVIC problem whose solution is known followed by concluding remarks and future work.

PROBLEM FORMULATION

Bolza Optimal Control Problem

Without loss of generality, consider the following general optimal control problem in Bolza form on the time interval $\tau \in [-1, +1]$; determine the state, $\mathbf{x}(\tau) \in \mathbb{R}^{n_x}$, the control, $\mathbf{u} \in \mathbb{R}^{n_u}$, the initial time, t_0, and the terminal time, t_f, that minimize the objective functional,

$$\mathcal{J} = \mathcal{M}(\mathbf{x}(-1), t_0, \mathbf{x}(+1), t_f) + \frac{t_f - t_0}{2} \int_{-1}^{+1} \mathcal{L}(\mathbf{x}(\tau), \mathbf{u}(\tau), \tau; t_0, t_f) \mathrm{d}\tau, \tag{1}$$

subject to the dynamic constraints,

$$\frac{\mathrm{d}\mathbf{x}}{\mathrm{d}\tau} = \frac{t_f - t_0}{2} \mathbf{a}(\mathbf{x}(\tau), \mathbf{u}(\tau), \tau; t_0, t_f), \tag{2}$$

the inequality path constraints,

$$\mathbf{c}_{\min} \leq \mathbf{c}(\mathbf{x}(\tau), \mathbf{u}(\tau), \tau; t_0, t_f) \leq \mathbf{c}_{\max}, \tag{3}$$

and the boundary conditions,

$$\mathbf{b}_{\min} \leq \mathbf{b}(\mathbf{x}(-1), t_0, \mathbf{x}(+1), t_f) \leq \mathbf{b}_{\max}. \tag{4}$$

Note, the independent variable $\tau \in [-1, +1]$ can be mapped back to the independent variable of the original optimal control problem $t \in [t_0, t_f]$ using the affine transformation,

$$t = \frac{t_f - t_0}{2}\tau + \frac{t_f - t_0}{2}. \tag{5}$$

Next, suppose that the domain $\tau \in [-1, +1]$ is partitioned into a mesh consisting of K mesh intervals $\mathcal{S}_k = [\tau_{k-1}, \tau_k]$, $k \in [1, ..., K]$, where $(\tau_0, ..., \tau_K)$ are the mesh points. Let $\mathbf{x}^{(k)}(\tau)$ and $\mathbf{u}^{(k)}(\tau)$ be the state and control, respectively, in the mesh interval $\mathcal{S}_k$, $k \in [1, ...K]$. The Bolza optimal control problem of Eqs.(1)-(4) can then be rewritten as follows; determine the state, $\mathbf{x}^{(k)}(\tau) \in \mathbb{R}^{n_x}$, the control, $\mathbf{u}^{(k)}(\tau) \in \mathbb{R}^{n_u}$, the initial time, t_0, and the final time, t_f, on the interval $\tau \in [-1, +1]$ that minimizes the objective functional,

$$\mathcal{J} = \mathcal{M}(\mathbf{x}^{(1)}(-1), t_0, \mathbf{x}^{(K)}(+1), t_f) + \frac{t_f - t_0}{2}\sum_{k=1}^{K}\int_{\tau_k}^{\tau_{k-1}} \mathcal{L}(\mathbf{x}^{(k)}(\tau), \mathbf{u}^{(k)}(\tau), \tau; t_0, t_f)\mathrm{d}\tau, \tag{6}$$

subject to the dynamic constraints,

$$\frac{\mathrm{d}\mathbf{x}^{(k)}(\tau)}{\mathrm{d}\tau} = \frac{t_f - t_0}{2}\mathbf{a}(\mathbf{x}^{(k)}(\tau), \mathbf{u}^{(k)}(\tau), \tau; t_0, t_f), \tag{7}$$

the inequality path constraints,

$$\mathbf{c}_{\min} \leq \mathbf{c}(\mathbf{x}^{(k)}(\tau), \mathbf{u}^{(k)}(\tau), \tau; t_0, t_f) \leq \mathbf{c}_{\max}, \tag{8}$$

and the boundary conditions,

$$\mathbf{b}_{\min} \leq \mathbf{b}(\mathbf{x}^{(1)}(-1), t_0, \mathbf{x}^{(K)}(+1), t_f) \leq \mathbf{b}_{\max}. \tag{9}$$

Since it is necessary that the state be continuous at the interior mesh points, the condition $\mathbf{x}(\tau_k^-) = \mathbf{x}(\tau_k^+)$ holds for $k = (1, ..., K-1)$.

Necessary Conditions for Optimality

The method developed in this research is based on the necessary conditions derived by Bryson, et. al.[14] and are given as follows. Suppose that the inequality path constraints given by Eq.(8) take on the following form,

$$\mathbf{c}(\mathbf{x}^{(k)}(\tau), \tau; t_0, t_f) \leq \mathbf{0}. \tag{10}$$

In order to determine a condition for the control when the equality in Eq.(10) holds, successive time derivatives of Eq.(10) are taken, and the dynamics $\mathbf{a}(\mathbf{x}(\tau), \mathbf{u}(\tau), \tau; t_0, t_f)$ is substituted for $\dot{\mathbf{x}}(\tau)$ until and expression explicit in the control is obtained. If q-derivatives are required, the state-variable inequality path constraints (SVICs) are deemed to be of q-th order. The Hamiltonian for the system then becomes,

$$\mathcal{H} = \mathcal{L} + \boldsymbol{\lambda}^{\mathsf{T}}\mathbf{a} + \boldsymbol{\mu}^{\mathsf{T}}\mathbf{c}^{(q)}, \tag{11}$$

where $\boldsymbol{\lambda}$ are the costate variables, and $\boldsymbol{\mu}$ is a set of Lagrange multipliers associated with the path constraints, $\mathbf{c}$, that satisfy the following necessary conditions,

$$\begin{array}{rcl} \boldsymbol{\mu} & \geq & \mathbf{0}, \text{ on the constraint boundary } (\mathbf{c} = \mathbf{0} \Rightarrow \mathbf{c}^{(q)} = \mathbf{0}), \\ \boldsymbol{\mu} & = & \mathbf{0}, \text{ off the constraint boundary } (\mathbf{c} < \mathbf{0}), \end{array} \tag{12}$$

where $\mathbf{c}^{(q)} = \mathrm{d}^{(q)}\mathbf{c}/\mathrm{d}t^{(q)}$. Then, the first-order optimality conditions resulting from the calculus of variations give,

$$\dot{\boldsymbol{\lambda}}^{\mathsf{T}} = -\frac{\partial \mathcal{H}}{\partial \mathbf{x}} = \begin{cases} -\dfrac{\partial \mathcal{L}}{\partial \mathbf{x}} - \boldsymbol{\lambda}^{\mathsf{T}}\dfrac{\partial \mathbf{a}}{\partial \mathbf{x}} - \boldsymbol{\mu}\dfrac{\partial \mathbf{c}^{(q)}}{\partial \mathbf{x}}, & \mathbf{c} = \mathbf{0}, \\ -\dfrac{\partial \mathcal{L}}{\partial \mathbf{x}} - \boldsymbol{\lambda}^{\mathsf{T}}\dfrac{\partial \mathbf{a}}{\partial \mathbf{x}}, & \mathbf{c} < \mathbf{0}. \end{cases} \tag{13}$$

In order to compute a finite control to keep the system on the constraint boundary, the path entering the constraint must satisfy the following *tangency* constraints:[14]

$$\mathbf{N}(\mathbf{x}(t_a), t_a) = \begin{bmatrix} \mathbf{c}(\mathbf{x}, t_a) \\ \mathbf{c}^{(1)}(\mathbf{x}, t_a) \\ \vdots \\ \mathbf{c}^{(q-1)}(\mathbf{x}, t_a) \end{bmatrix} = \mathbf{0}, \quad q = 1, 2, ... \tag{14}$$

where t_a is the time at which the constraint becomes active. It has been shown in[26] that when a constraint is active, the index of the original system of differential algebraic equations (DAEs) increases. In a direct method, enforcing Eq.(14) is analogous to performing index reduction. Specifically, the tangency constraints provide a set of necessary conditions that reduce the index of the constrained system of DAEs to the index of the unconstrained system.

MULTIPLE-DOMAIN LEGENDRE-GAUSS-RADAU COLLOCATION

The method developed in this paper utilizes Legendre-Gauss-Radau (LGR) collocation to discretize the continuous Bolza optimal control problem. The LGR collocation method is chosen due to its ability to converge to a solution at an exponential rate when the solution is smooth.[8] However, for the problems studied in this research, the solution may be nonsmooth due to active state-constrained arcs. Consequently, in order to be able to correctly enforce the tangency constraints and handle potential nonsmooth behavior, the method developed in this research utilizes a multiple-domain LGR collocation method (similar to Pager, et. al.[28]) described below,

Multiple-Domain Formulation

Let the horizon $t \in [t_0, t_f]$ of the Bolza optimal control problem be partitioned into D domains, $\mathcal{P}_d = [t_s^{\{d-1\}}, t_s^{(s)}] \subseteq [t_0, t_f]$, $d \in [1, ..., D]$, such that,

$$\begin{array}{rcl} \bigcup_{d=1}^{D} \mathcal{P}_d & = & [t_0, t_f], \\ \bigcap_{d=1}^{D} \mathcal{P}_d & = & [t_s^{\{1\}}, ..., t_s^{\{D-1\}}], \end{array} \tag{15}$$

where $t_s^{\{d\}}$, are the *domain interface variables*, $t_s^{\{0\}} = t_0$, $t_s^{\{D\}} = t_f$, are the initial and final times, respectively, d is the domain index, and s is signifies a switch between a constrained or unconstrained arc. Specifically, for the method developed in this research, $t_s^{\{d\}}$ correspond to switches in activation and deactivation of the state-variable inequality constraint, whereas in Pager, et. al.,[28] these variables serve as switch points in bang-bang and/or singular control structures. It is noted that the domain interface variables become additional decision variables in the resulting nonlinear programming problem (NLP) and are *not* collocation points.

Similar to the formulation presented before, each domain $\mathcal{P}_d = [t_s^{\{d-1\}}, t_s^{(s)}]$ is mapped to $\tau \in [-1, +1]$ using the affine transformation,

$$t = \frac{t_s^{(d)} - t_s^{(d-1)}}{2}\tau + \frac{t_s^{(d)} - t_s^{(d-1)}}{2} \tag{16}$$

Next, the time interval $\tau \in [-1, +1]$ on each domain is divided into K mesh intervals, $\mathcal{S}_k = [T_{k-1}, T_k] \subseteq [-1, +1]$, for $k = [1, ..., K]$, such that,

$$\begin{array}{rcl} \bigcup_{k=1}^{K} \mathcal{S}_k & = & [\tau_0, \tau_f], \\ \bigcap_{k=1}^{K} \mathcal{S}_k & = & [T_1, ..., T_{K-1}]. \end{array} \tag{17}$$

Legendre-Gauss-Radau Collocation

Once the multiple-domain formulation is complete, LGR collocation is used to discretize the continuous time problem on each mesh interval. Specifically, for each mesh interval, the LGR points are defined on $[T_{k-1}, T_k] \subseteq [-1, +1]$, $k = [1..., K]$. The state of the continuous time optimal control problem is then approximated within each mesh interval $\mathcal{S}_k$ by,

$$\mathbf{x}^{(k)}(\tau) \approx \mathbf{X}^{(k)}(\tau) = \sum_{j=1}^{N_k+1} \mathbf{X}_j^{(k)} \ell_j^{(k)}(\tau), \tag{18}$$

where $\ell_j^{(k)}(\tau)$, $j = [1, ..., N_k + 1]$, is a basis of Lagrange polynomials on S_k given by,

$$\ell_j^{(k)}(\tau) = \prod_{\substack{i=1 \\ i \neq j}}^{N_k+1} \frac{\tau - \tau_i^{(k)}}{\tau_j^{(k)} - \tau_i^{(k)}}, \tag{19}$$

where $(\tau_1^{(k)}, ..., \tau_{N_k}^{(k)})$ are the N_k set of LGR collocation points in the interval $[T_{k-1}, T_k)$, with $\tau_{N_k+1} = T_k$ being a non-collocated support point. Differentiating Eq.(18) with respect to τ leads to,

$$\frac{\mathrm{d}\mathbf{X}^{(k)}(\tau)}{\mathrm{d}\tau} = \sum_{j=1}^{N_k+1} \mathbf{X}_j^{(k)} \frac{\mathrm{d}\ell_j^{(k)}(\tau)}{\mathrm{d}\tau}. \tag{20}$$

The dynamic constraints given in Eq.(7) are then approximated at the N_k-LGR points in mesh interval $\mathcal{S}_k$, $k = [1, ..., K]$ on domain $d = [1, ..., D]$ by,

$$\sum_{j=1}^{N_k+1} D_{ij}^{(k)} \mathbf{X}_j^{(k)} - \frac{t_f - t_0}{2} \mathbf{a}\left(\mathbf{X}_i^{(k)}, \mathbf{U}_i^{(k)}, t(\tau_i^{(k)}, t_s^{\{d-1\}}, t_s^{\{d\}})\right) = 0, \;\; \forall i \in \{1, ..., N_k\} \tag{21}$$

where,

$$D_{ij}^{(k)} = \frac{\mathrm{d}\ell_j^{(k)}(\tau)}{\mathrm{d}\tau}, \;\; \forall i \in \{1, ..., N_k\}, \forall j \in \{1, ..., N_k + 1\} \tag{22}$$

are the elements of the $N_k \times (N_k + 1)$ Legendre-Gauss-Radau *differentiation matrix* in the mesh interval $\mathcal{S}_k$, and $\mathbf{U}_i^{(k)}$ is the approximation of the control at the i-th collocation point in mesh interval $\mathcal{S}_k$. Continuity in the state across mesh intervals $\mathcal{S}_{k-1}, \mathcal{S}_k$ and time domains $\mathcal{P}_{d-1}, \mathcal{P}_d$ is achieved by using the same variable to represent $\mathbf{X}_{N_{k-1}+1}^{k-1} = \mathbf{X}_1^{(k)}$ and $\mathbf{X}_{N^{\{d-1\}}+1}^{\{d-1\}} = \mathbf{X}_1^{\{d\}}$, respectively. Lastly, it is noted that $N^{\{d\}}$ is the total number of collocation points in the time domain $\mathcal{P}_d$ and can be computed by,

$$N^{\{d\}} = \sum_{k=1}^{K^{\{d\}}} N_k^{\{d\}} \tag{23}$$

where $K^{\{d\}}$ is the total number of mesh intervals in time domain $\mathcal{P}_d$, $d = \{1, ..., D\}$.

Nonlinear Programming Problem

The multiple-domain Legendre-Gauss-Radau (LGR) discretization of the continuous time multiple-domain Bolza optimal control problem results in a large sparse nonlinear programming (NLP) which is given as follows. Minimize the objective functional,

$$\mathcal{J} = \mathcal{M}\left(\mathbf{X}_1^{\{1\}}, t_0, \mathbf{X}_{N^{\{D\}}+1}^{\{D\}}, t_f\right) + \sum_{d=1}^{D} \frac{t_s^{\{d\}} - t_s^{\{d-1\}}}{2} \left[\mathbf{w}^{\{d\}}\right]^{\mathsf{T}} \mathbf{L}^{\{d\}}, \tag{24}$$

subject to the dynamic constraints,

$$\boldsymbol{\Delta}^{\{d\}} = \mathbf{D}^{\{d\}}\mathbf{X}^{\{d\}} - \frac{t_s^{\{d\}} - t_s^{\{d-1\}}}{2}\mathbf{A}^{\{d\}} = \mathbf{0}, \ \ \forall d \in \{1, ..., D\}, \tag{25}$$

the inequality path constraints,

$$\mathbf{c}_{\text{min}} \leq \mathbf{C}_j^{\{d\}} \leq \mathbf{c}_{\text{max}}, \ \ \forall j \in \{1, ..., N^{\{d\}}\}, \ \ \forall d \in \{1, ..., D\}, \tag{26}$$

the boundary conditions,

$$\mathbf{b}_{\text{min}} \leq \mathbf{b}\left(\mathbf{X}_1^{\{1\}}, t_0, \mathbf{X}_{N^{\{d\}}+1}^{\{d\}}, t_f\right) \leq \mathbf{b}_{\text{max}}, \tag{27}$$

and the continuity conditions,

$$\mathbf{X}_{N^{\{d-1\}}+1}^{\{d-1\}} = \mathbf{X}_1^{\{d\}}, \tag{28}$$

where $\mathbf{D}^{\{d\}} \in \mathbb{R}^{N^{\{d\}} \times (N^{\{d\}}+1)}$ is the LGR differentiation matrix in the time domain $\mathcal{P}_d$, $d = [1, ..., D]$, and $\mathbf{w}^{\{d\}} \in \mathbb{R}^{N^{\{d\}} \times 1}$ are the LGR weights at each collocation point in the time domain $\mathcal{P}_d$. Note, the continuity conditions in Eq. (28) are implicitly enforced by using the same decision variable in the NLP for $\mathbf{Y}_{N^{\{d-1\}}+1}^{\{d-1\}}$ and $\mathbf{Y}_1^{\{d\}}$.

STRUCTURE DETECTION METHOD

The overall method used in this research aims to automatically decompose the original inequality constrained optimal control problem into a multiple-domain optimal control problem consisting of state constrained and unconstrained domains. Partitioning the problem into multiple domains provides the ability to apply the higher order necessary tangency conditions at the beginning of constrained domains. The multiple-domain formulation also allows the resulting mixed state-control equality constraint (highest time derivative of the path constraint that contains the control) to be enforced throughout constrained domains. Applying the higher order necessary conditions reduces the high-index system of differential algebraic equations (DAEs), and provides the capability to accurately approximate the control while any state-variable inequality constraints (SVICs) are active.

The first step in partitioning the problem is to obtain an estimate of the domain interface variables, which are analogous to activation/deactivation (A/D) times of any SVICs. Before presenting the structure detection method (SDM) for estimating the domain interface variables, the following assumptions are made in the development of the algorithm:

Assumption 1: The SVICs are not active at the start of the trajectory: $\mathbf{c}(\mathbf{x}(t_0), t_0) < \mathbf{0}$.

Assumption 2: The SVICs are not active at the end of the trajectory: $\mathbf{c}(\mathbf{x}(t_f), t_f) < \mathbf{0}$.

The above assumptions are in place to be able to inspect neighboring collocation points to determine the activation or deactivation of constrained arcs. It is noted that in Jacobson, et. al.,[15] a set of new necessary conditions were derived which show that, in certain cases, for SVICs of *odd* order ($q > 1$), the state may *not* be constrained over a non-zero interval of time, but instead only touch the constraint boundary at a single point. This occurrence is often referred to as a *touch point*. It is mentioned here that the structure detection method developed in this research is for SVICs that contain constrained arcs over non-zero intervals of time. That is, the potential existence of touch points are not studied in this research. The SDM begins by computing an approximate solution on a single domain $\mathcal{P}_1 = [t_0, t_f]$ using standard Legendre-Gauss-Radau (LGR) collocation on a fixed mesh consisting of S_k, $k = [1, ...K]$ mesh intervals with N_k number of collocation points within each mesh interval. Next, let $\mathbf{X}(\tau_j^{(k)})$, $j = [1, ..., N_k + 1]$, be the approximated state solution obtained on the initial domain at the j^{th} collocation point in the k^{th} mesh interval, then the following relative difference is computed at every collocation point plus the final non-collocated point for every SVIC in the problem,

$$\delta c_i(\tau_j^{(k)}) = \frac{\left|c_i(\mathbf{X}(\tau_j^{(k)}), \tau_j^{(k)}) - c_{i,\max}\right|}{1 + |c_{i,\max}|}, \quad \forall j \in \{1, ..., N_k + 1\}, \forall k \in \{1, ..., K\} \tag{29}$$

where c_i is the i-th SVIC for all $i = [1, ..., n_c]$ with n_c being the total number of SVICs. Once the relative difference in Eq.(29) is obtained at every collocation point plus the final non-collocated point, the structure detection algorithm for estimating the activation/deactivation points is executed as follows:

Detection Method for State-Variable Inequality Constrained Optimal Control Problems

Step 1: Set detection tolerance for which renders a constraint active: ϵ.

Step 2: Check relative difference to determine activation/deactivation points: $\forall\ j \neq \{1, N_{K+1}\}$, $\forall k \neq \{1, K\}$

(a): If $\delta c_i(\tau_j^{(k)}) \leq \epsilon$, and

(i): $\delta c_i(\tau_{j-1}^{(k)}) > \epsilon$, and $\delta c_i(\tau_{j+1}^{(k)}) \leq \epsilon$, then $\tau_j^{(k)}$ is deemed an *activation* point.

(ii): $\delta c_i(\tau_{j-1}^{(k)}) \leq \epsilon$, and $\delta c_i(\tau_{j+1}^{(k)}) > \epsilon$, then $\tau_j^{(k)}$ is deemed a *deactivation* point.

Step 3: Compute bounds on estimated activation/deactivation points: $\left(\tau_j^{(k)}\right)^{\pm}$

The default detection tolerance (ϵ) that is used in the detection algorithm is chosen such that it follows a process analogous to selecting the NLP solver tolerance. Specifically, the NLP tolerance is typically chosen to be on the order of the square root of machine tolerance ($\sim \mathcal{O}(10^{-8})$), and so the default detection tolerance is chosen similarly to be on the order of the square root of the NLP solver tolerance ($\sim \mathcal{O}(10^{-4})$) given the solution on the initial mesh is governed by the accuracy at which the NLP solver can achieve. A graphical example of step 2 in the detection algorithm is provided below in Fig. 1. Lastly, it is noted that the final step in the detection algorithm is performed because the detected A/D times are included as additional decision variables in the resulting nonlinear programming problem (NLP) and must be bounded to prevent overlapping or collapsing of domains within the partitioned problem. The bounds are obtained by,

$$\begin{aligned} \left(\tau_j^{(k)}\right)^{-} &= \tau_j^{(k)} + \nu \left(\tau_{j-1}^{(k)} - \tau_j^{(k)}\right), \\ \left(\tau_j^{(k)}\right)^{+} &= \tau_j^{(k)} + \nu \left(\tau_{j+1}^{(k)} - \tau_j^{(k)}\right), \end{aligned} \tag{30}$$

where $\nu > 0$ is a user defined parameter used to control the size of the allowable search space for the NLP solver to determine the optimal A/D times. Once estimates of the domain interface variables are obtained, the original optimal control problem is partitioned into a multiple-domain optimal control problem consisting of constrained and unconstrained domains. Next, the multiple-domain continuous time optimal control problem is transcribed into a large sparse NLP using the multiple-domain LGR collocation scheme presented in the previous section. Also, it is noted here again for clarity, the estimated A/D times obtained from the detection algorithm are appended to the NLP decision vector to be optimized when solving the resulting NLP. At the start of each identified constrained domain, the necessary tangency conditions given by Eq.(14) are enforced. Additionally, the q-th time derivative of any detected state-variable inequality constraints is applied as an equality constraint throughout constrained domains, while throughout unconstrained domains, the state-variable inequality constraints are applied in their original form.

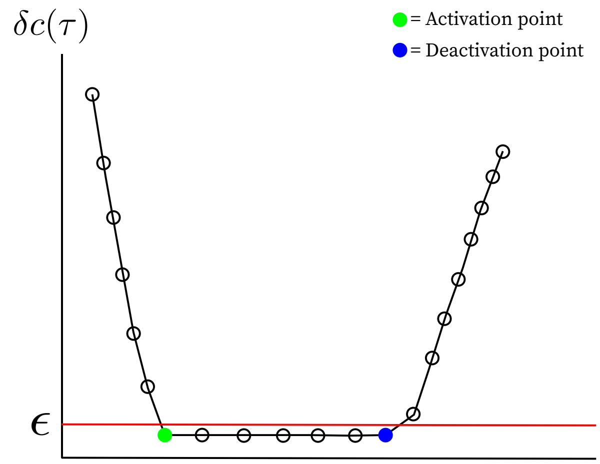

Figure 1: Example for detecting activation/deactivation points in a SVIC.

NUMERICAL EXAMPLE

To illustrate the accuracy of the method present in this paper, a benchmark optimal control problem with a single state-variable inequality path constraint (SVIC) is solved. This example problem, often referred to as the Bryson-Denham problem,[14] was chosen due to the fact that it has a known analytical solution, which provides a baseline to analyze the accuracy of the proposed method presented in this paper. The Bryson-Denham problem is given as follows;[14] minimize the objective functional,

$$\mathcal{J} = \frac{1}{2}\int_0^1 u^2(t)\mathrm{d}t, \tag{31}$$

subject to the dynamic constraints,

$$\begin{aligned} \dot{x}(t) &= v(t), \\ \dot{v}(t) &= u(t), \end{aligned} \tag{32}$$

the boundary conditions,

$$\begin{array}{rcrcl} x(0) &=& x(1) &=& 0, \\ v(0) &=& -v(1) &=& 1, \end{array} \tag{33}$$

and the pure state-variable inequality constraint,

$$x(t) \leq L, \tag{34}$$

where L is the upper limit on the SVIC. Though the problem formulation may appear rudimentary, it is challenging to obtain an accurate numerical approximation of the solution. For completeness, the analytical solution to the above optimal control for $0 \leq L \leq 1/6$ is found to be,

$$u^*(t) = \begin{cases} -\dfrac{2}{3L}\left(1 - \dfrac{t}{3L}\right), & 0 \leq t \leq 3L \\ 0, & 3L \leq t \leq 1 - 3L \\ -\dfrac{2}{3L}\left(1 - \dfrac{1-t}{3L}\right), & 1 - 3L \leq t \leq 1 \end{cases} \tag{35}$$

$$v^*(t) = \begin{cases} \left(1 - \dfrac{t^2}{3L}\right), & 0 \leq t \leq 3L \\ 0, & 3L \leq t \leq 1 - 3L \\ -\left(1 - \dfrac{1-t}{3L}\right)^2, & 1 - 3L \leq t \leq 1 \end{cases} \tag{36}$$

$$x^*(t) = \begin{cases} L\left[1 - \left(1 - \dfrac{t}{3L}\right)^3\right], & 0 \leq t \leq 3L \\ L, & 3L \leq t \leq 1 - 3L \\ L\left[1 - \left(1 - \dfrac{1-t}{3L}\right)^3\right], & 1 - 3L \leq t \leq 1 \end{cases} \tag{37}$$

$$\mathcal{J}^* = \frac{4}{9L} \tag{38}$$

For the results to follow, the upper limit on the SVIC was chosen to be $L = 1/9 \Rightarrow \mathcal{J}^* = 4$. The resulting nonlinear programming problem (NLP) was solved using the NLP solver *IPOPT* with a solver tolerance of 1×10^{-8}. The NLP was solved in full-Newton mode, and the required derivatives to be provided to the NLP solver were obtained using sparse central-differencing. All computations were performed on a 2.9 GHz Intel Core i9 MacBook Pro running macOS Monterey Version 12.5 with 32 GB 2400 MHz DDR4 of RAM, using MATLAB version R2021a (build 9.10.0.1669831). The initial static mesh for obtaining an approximate

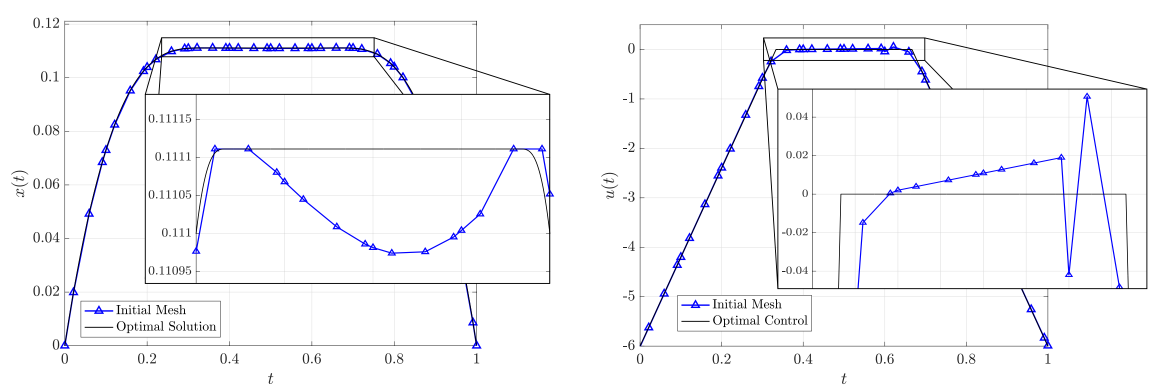

(a) Position, $x(t)$ vs. time, t.

(b) Control, $u(t)$ vs. time, t.

Figure 2: Computed position, $x(t)$, and control, $u(t)$, on the initial static mesh with $K = 10$, $N_k = 4$.

solution on a single domain (which is used to perform structure detection) was chosen to consist of $K = 10$ mesh intervals and $N_k = 4$ collocation points within each mesh. Figure 2 shows the computed position, $x(t)$, and control, $u(t)$, on the initial static mesh. Upon zooming in on the portion of the solution which contains

the constrained arc, $x(t) = L$, it is observed that the computed position does not remain along the constraint boundary (as shown in Fig 2a), and contains large "jumps" or "chattering" in the control (as shown in Fig. 2b). Next, Fig 3 provides a comparison between the approximate solution obtained on the initial mesh and a solution obtained using an hp-adaptive direct collocation method[11] implemented in the MATLAB optimal control software $\mathbb{GPOPS}-\mathbb{II}$,[29] referred to as hp-LGR. Specifically, Fig 3 shows the computed position, $x(t)$, and control, $u(t)$, using the hp-LGR method alongside the solution on the initial mesh. Two observations can be made from Fig. 3, first being that the hp-LGR method places more collocation points near the activation and deactivation of the SVIC. Secondly, the hp-LGR method is able to obtain a position which is tighter to the constraint boundary, but still fails to remain on the boundary throughout the constrained arc. Additionally, the hp-LGR method obtains a control profile which reduces the magnitude of the chattering behavior, but still appears to be present near the activation and deactivation of the constraint. While in general advanced hp-adaptive methods can improve accuracy when path constraints are present, they still may return poor solutions when a pure state-variable inequality constraint is present.
Lastly, the solutions obtained on the initial mesh and with the hp-LGR method are compared against the solution computed using the structure detection method (SDM) developed in this paper. As previously mentioned, the SDM utilizes the solution on the initial mesh (shown in Fig. 2) to obtain estimates of the activation/deactivation (A/D) times of the SVIC before partitioning the problem into multiple domains. Using

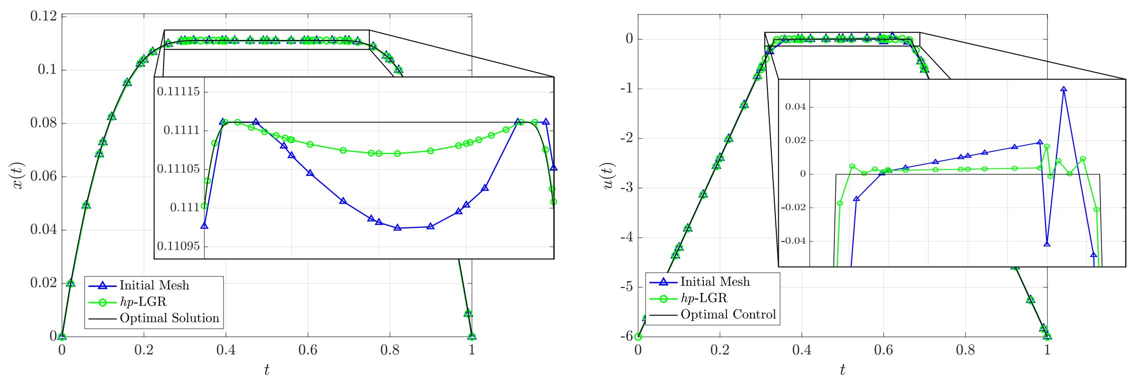

(a) Position, $x(t)$ vs. time, t.

(b) Control, $u(t)$ vs. time, t.

Figure 3: Computed position, $x(t)$, and control, $u(t)$, using an hp-adaptive direct collocation method.

a detection tolerance of $\epsilon \sim \mathcal{O}(10^{-4})$, Table 1 provides the estimated A/D times $\hat{t}_s$, the lower and upper bounds $\hat{t}_s^-$,$\hat{t}_s^+$, respectively, the optimized A/D times t_s returned by the nonlinear programming problem (NLP) solver, and the known analytic switch times. By comparing the estimated and optimized switch times with the analytical switch times, it is observed that the optimizer is capable of selecting switch times closer to the known A/D times. Figure 4 shows the solution obtained using the SDM alongside the solution obtained on the initial mesh and that obtained using the hp-LGR method. Note, the vertical dashed lines appearing in

Switch time	$\hat{t}_s$	$\hat{t}_s^-$	$\hat{t}_s^+$	t_s	Analytic
Activation	0.300000	0.255706	0.406170	0.333326	1/3
Deactivation	0.700000	0.655706	0.806170	0.666672	2/3

Table 1: Estimated activation/deactivation times, $\hat{t}_s$, lower and upper bounds $\hat{t}_s^-, \hat{t}_s^+$ (obtained with Eq.(30) and $\nu = 5$), and optimized activation/deactivation times t_s

Fig. 4 represent the optimized activation/deactivation times returned by the NLP solver. Figure 4a shows that the SDM is capable of computing a position that is much tighter to the constraint boundary throughout the constrained arc. Furthermore, Fig. 4b shows that the SDM returns a control profile which completely removes any chattering behavior. Table 2 displays the computed relative errors with respect to the known analytical

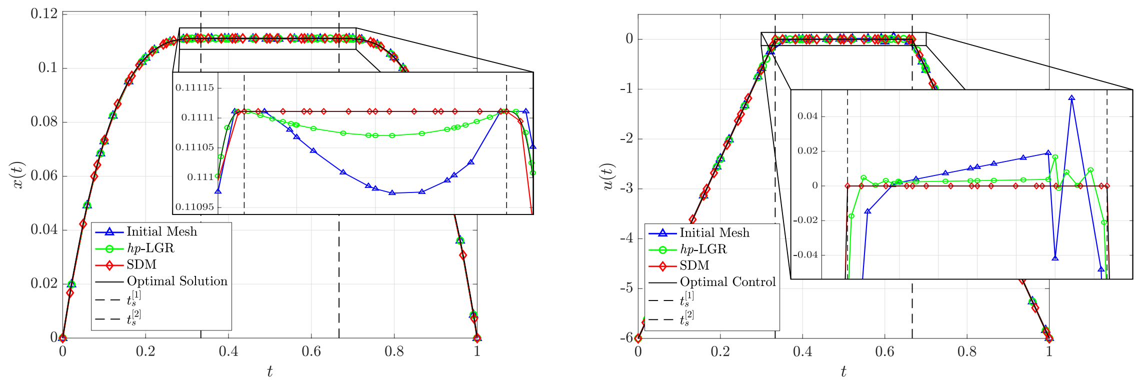

(a) Position, $x(t)$ vs. time, t.

(b) Control, $u(t)$ vs. time, t.

Figure 4: Computed position, $x(t)$, and control, $u(t)$, using the structure detection method (SDM).

solution in the objective value, $\mathcal{J}$, the activation time, $t_s^{[1]}$, and the deactivation time, $t_s^{[2]}$, for each solution studied. It is observed that the SDM is capable of computing an objective that is eight orders of magnitude more accurate than the objective obtained using the hp-LGR method. Additionally, an improvement of up to four orders of magnitude in the computed A/D times is obtained when using the SDM.

Relative Error	Objective Value ($\mathcal{J}$)	Activation Time ($t_s^{[1]}$)	Deactivation Time ($t_s^{[2]}$)
Initial Mesh	8.689017E-05	3.629784E-02	1.142003E-02
hp-LGR	1.245222E-05	2.884690E-02	1.785373E-02
SDM	1.494360E-13	4.535400E-05	5.579097E-06

Table 2: Relative error of the computed cost and activation/deactivation times with respect to the analytical solution for the initial mesh, hp-LGR method, and structure detection method (SDM).

CONCLUSION

A structure detection method for solving state-variable inequality path constrained (SVIC) optimal control problems using a multiple-domain Legendre-Gauss-Radau (LGR) collocation method has been developed. The method obtains estimates of activation/deactivation times in SVICs, and introduces the detected times as additional decision variables in the resulting nonlinear program (NLP). Based on the number of detected times, the method automatically partitions the problem into constrained and unconstrained domains. Lastly, the necessary tangency conditions are applied at the start of constrained domains, and the appropriate time derivative of the SVICs are enforced as equality constraints. By analyzing a well-known SVIC optimal control problem, it has been shown that the structure detection method developed in this research computes an approximation to the solution of much higher accuracy than that obtained with an hp-LGR adaptive collocation method. The results of this research show the benefit for including higher order necessary conditions in the problem formulation as well as allowing the optimizer to select the best location for when the constraints become active/deactive. Future work will aim towards solving more challenging SVIC optimal control problems, including those that may contain touch points and/or multiple state-variable inequality path constraints.

REFERENCES

[1] A. V. Rao, "Survey of Numerical Methods for Optimal Control," *Proceedings of the Astrodynamics Specialist Conference*, Pittsburgh, PA, AAS Paper 09-334, August 10-12, 2009.

[2] L. T. Biegler and V. M. Zavala, "Large-Scale Nonlinear Programming Using IPOPT: An Integrating Framework for Enterprise-Wide Optimization," *Computers and Chemical Engineering*, Vol. 33, March 2008, pp. 575–582.

[3] P. E. Gill, W. Murray, and M. A. Saunders, "SNOPT: An SQP Algorithm for Large-Scale Constrained Optimization," *SIAM Review*, Vol. 47, January 2002, pp. 99–131.

[4] D. A. Benson, G. T. Huntington, T. P. Thorvaldsen, and A. V. Rao, "Direct Trajectory Optimization and Costate Estimation via an Orthogonal Collocation Method," *Journal of Guidance, Control, and Dynamics*, Vol. 29, November-December 2006, pp. 1435–1440.

[5] S. Kameswaran and L. T. Biegler, "Convergence Rates for Direct Transcription of Optimal Control Problems Using Collocation at Radau Points," *Computational Optimization and Applications*, Vol. 41, No. 1, 2008, pp. 81–126.

[6] D. Garg, M. A. Patterson, W. W. Hager, A. V. Rao, D. A. Benson, and G. T. Huntington, "A Unified Framework for the Numerical Solution of Optimal Control Problems Using Pseudospectral Methods," *Automatica*, Vol. 46, November 2010, pp. 1843–1851. DOI: 10.1016/j.automatica.2010.06.048.

[7] G. Elnagar, M. A. Kazemi, and M. Razzaghi, "The Pseudospectral Legendre Method for Discretizing Optimal Control Problems," *IEEE transactions on Automatic Control*, Vol. 40, No. 10, 1995, pp. 1793–1796.

[8] H. Hou, W. Hager, and A. Rao, "Convergence of a Gauss Pseudospectral Method for Optimal Control," *AIAA Guidance, Navigation, and Control Conference*, American Institute of Aeronautics and Astronautics, aug 2012, 10.2514/6.2012-4452.

[9] C. L. Darby, W. W. Hager, and A. V. Rao, "An hp–Adaptive Pseudospectral Method for Solving Optimal Control Problems," *Optimal Control Applications and Methods*, Vol. 32, No. 4, 2011, pp. 476–502.

[10] C. L. Darby, W. W. Hager, and A. V. Rao, "Direct Trajectory Optimization Using a Variable Low-Order Adaptive Pseudospectral Method," *Journal of Spacecraft and Rockets*, Vol. 48, May–June 2011, pp. 433–445.

[11] M. A. Patterson, W. W. Hager, and A. V. Rao, "A ph Mesh Refinement Method for Optimal Control," *Optimal Control Applications and Methods*, Vol. 36, July–August 2015, pp. 398–421.

[12] F. Liu, W. W. Hager, and A. V. Rao, "Adaptive mesh refinement method for optimal control using nonsmoothness detection and mesh size reduction," *Journal of the Franklin Institute*, Vol. 352, oct 2015, pp. 4081–4106, 10.1016/j.jfranklin.2015.05.028.

[13] F. Liu, W. W. Hager, and A. V. Rao, "Adaptive Mesh Refinement for Optimal Control Using Nonsmoothness Detection and Mesh Size Reduction," *IEEE Transactions on Control System Technology*, Vol. Published Online in Early View, June 2017, pp. 4081–4106.

[14] A. E. Bryson, W. F. Denham, and S. E. Dreyfus, "Optimal Programming Problems with Inequality Constraints I: Necessary Conditions for Extremal Solutions," *AIAA Journal*, Vol. 1, November 1963, pp. 2544–2550.

[15] D. Jacobson, M. Lele, and J. Speyer, "New necessary conditions of optimality for control problems with state-variable inequality constraints," *Journal of Mathematical Analysis and Applications*, Vol. 35, No. 2, 1971, pp. 255–284, 10.1016/0022-247X(71)90219-8.

[16] E. Kreindler, "Additional necessary conditions for optimal control with state-variable inequality constraints," *Journal of Optimization Theory and Applications*, Vol. 38, 1982, pp. 241–250.

[17] R. F. Hartl, S. Sethi, and R. Vickson, "A Survey of the Maximum Principles for Optimal Control Problems with State Constraints," *SIAM Review*, Vol. 37, No. 2, 1995, pp. 181–218.

[18] P. Liu, X. Li, X. Liu, and Y. Hu, "An improved smoothing technieque-based control vector parameterization method for optimal control problems with inequality path constraints," *Journal of Optimal Control Applications and Methods*, Vol. 38, aug 2016, pp. 586–600, 10.1002/oca.2273.

[19] K. Mall, M. J. Grant, and E. Taheri, "Uniform Trigonometrization Method for Optimal Control Problems with Control and State Constraints," *Journal of Spacecraft and Rockets*, Vol. 57, sep 2020, pp. 995–1007, 10.2514/1.A34624.

[20] C. R. Heidrich, M. J. Sparapany, and M. J. Grant, "Generalized Regularization of Constrained Optimal Control Problems," *Journal of Spacecraft and Rockets*, jan 2021, 10.2514/1.A35229.

[21] D. Jacobson and M. Lele, "A transformation technique for optimal control problems with a state variable inequality constraint," *IEEE Transactions on Automatic Control*, Vol. 14, 1969, pp. 457–464, 10.1109/TAC.1969.1099283.

[22] K. Graichen and N. Petit, “Incorporating a class of constraints into the dynamics of optimal control problems,” *Journal of Optimal Control Applications and Methods*, Vol. 30, jan 2009, pp. 537–561, 10.1002/oca.880.

[23] B. C. Fabien, “Indirect Solution of Inequality Constrained and Singular Optimal Control Problems Via a Simple Continuation Method,” *Journal of Dynamic Systems, Measurement, and Control*, Vol. 136, nov 2013, p. 021003, 10.1115/1.4025596.

[24] S. E. Dreyfus, “Variational problems with inequality constraints,” *Journal of Mathematical Analysis and Applications*, Vol. 4, 1962, pp. 297–308.

[25] W. F. Denham and A. E. Bryson, “Optimal Programming Problems with Inequality Constraints II: Solution by Steepest-Ascent,” *AIAA Journal*, Vol. 2, January 1964, pp. 25–34.

[26] W. F. Feehery and P. I. Barton, “Dynamic optimization with state variable path constraints,” *Computers & Chemical Engineering*, Vol. 22, No. 9, 1998, pp. 1241–1256, https://doi.org/10.1016/S0098-1354(98)00012-X.

[27] S. Kameswaran and L. T. Biegler, “Advantages of Nonlinear-Programming-Based Methodologies for Inequality Path-Constrained Optimal Control Problems—A Numerical Study,” *SIAM Journal on Scientific Computing*, Vol. 30, No. 2, 2008, pp. 957–981, 10.1137/050644938.

[28] E. R. Pager and A. V. Rao, “Method for solving bang-bang and singular optimal control problems using adaptive Radau collocation,” *Computational Optimization and Applications*, jan 2022, pp. 857–887, 10.1007/s10589-022-00350-6.

[29] M. A. Patterson and A. V. Rao, “GPOPS-II: A MATLAB Software for Solving Multiple-Phase Optimal Control Problems Using hp-Adaptive Gaussian Quadrature Collocation Methods and Sparse Nonlinear Programming,” *ACM Transactions on Mathematical Software*, Vol. 41, oct 2014, pp. 1–37, 10.1145/2558904.